

FINAL REPORT  
REMOTE DETECTION OF  
TRAILING VORTICES

ER71-4233

17 June 1971

Reproduced by  
NATIONAL TECHNICAL  
INFORMATION SERVICE  
US Department of Commerce  
Springfield, VA. 22151



N72-12375 (NASA-CR-121034) REMOTE DETECTION OF  
TRAILING VORTICES, TASK 3, MODIFICATION 3  
Final Report J. Fridman, et al (Raytheon  
Co.) 17 Jun. 1971 29 p CSCL 14B

Unclas  
09340

G3/14

FINAL REPORT  
REMOTE DETECTION OF  
TRAILING VORTICES

ER71-4233

17 June 1971

TASK III, MODIFICATION NO.3  
of  
CONTRACT NAS8-30512

Prepared for  
GEORGE C. MARSHALL SPACE FLIGHT CENTER  
NASA

Huntsville, Alabama 35812

Prepared by

J. Fridman  
C. Harris  
A. Jelalian  
Dr. W. Keene  
K. Meister  
C. Miller  
Dr. C. Sonnenschein

RAYTHEON COMPANY  
ADVANCED DEVELOPMENT LABORATORIES  
EQUIPMENT DIVISION

Sudbury, Massachusetts 01776



CONTENTS

<u>SECTION</u>		<u>PAGE</u>
1	INTRODUCTION . . . . .	1-1
2	FIELD MEASUREMENTS AND DATA ANALYSIS . . . . .	2-1
2.1	Measurements at Marshall Space Flight Center. . . . .	2-1
2.1.1	July, 1970. . . . .	2-1
2.1.2	September - November, 1970. . . . .	2-1
2.1.2.1	Measurements. . . . .	2-1
2.1.2.2	Laser Beam Profile and Lens Matching. . . . .	2-1
2.1.2.3	LDV Resolution Data . . . . .	2-3
2.1.3	December, 1970. . . . .	2-5
2.2	Measurements at Colorado State University Site . . . . .	2-5
2.2.1	February, 1971. . . . .	2-5
2.2.2	March - April, 1971. . . . .	2-7
3	GROUND WINDS FREQUENCY TRACKER . . . . .	3-1
3.1	Characteristics . . . . .	3-1
3.2	Operation of the Model 12C Frequency Tracker . . . . .	3-7
4	CONCLUSIONS AND RECOMMENDATIONS. . . . .	4-1



ILLUSTRATIONS

<u>FIGURE</u>		<u>PAGE</u>
2-1	Range Resolution (f - 73 feet) . . . . .	2-6
2-2	Signal Returns from Spinning Disks. . . . .	2-8
2-3	Snow Returns at Various Ranges, 12-Inch Transmitter . . . . .	2-10
2-4	Snow Returns at Various Ranges, 12-Inch System with 6-Inch Aperture. . . . .	2-11
2-5	Ground Wind Returns, Ft. Collins, Colorado 31 March 1971 . . . . .	2-12
3-1	Foster-Seely Discriminator S-Characteristic . . .	3-4
3-2	Wide Filter/Original Discriminator, Discriminator Zero Not Adjusted . . . . .	3-5
3-3	Wide Filter/Realigned Discriminator with Zero Adjustment. . . . .	3-5
3-4	Narrow Filter/Realigned Discriminator with Zero Adjustment. . . . .	3-6
3-5	4.3 ft/second Ground Wind Signal. . . . .	3-8
3-6	3.3 ft/second Ground Wind Signal. . . . .	3-9
3-7	2.7 ft/second Ground Wind Signal. . . . .	3-10
3-8	2.3 ft/second Ground Wind Signal. . . . .	3-11

SECTION 1

INTRODUCTION

This is the final report for Task III of the Remote Detection of Trailing Vortices Program (Contract No. NAS8-30512, Modification No.3).

This contract task had two primary aims:

- (1) Design and construct a frequency tracker for use with the Laser Doppler Velocimeter.
- (2) Provide technical assistance to operate the one-dimensional LDV at Marshall Space Flight Center and Colorado State University.

The operating characteristics and operation of the frequency tracker are described in Section 3. A more detailed operating manual has been supplied under separate cover.

Section 2 describes the measurements which were made during the program and some of the operating characteristics of the LDV.

SECTION 2

FIELD MEASUREMENTS AND DATA ANALYSIS

2.1 MEASUREMENTS AT MARSHALL SPACE FLIGHT CENTER

2.1.1 JULY, 1970

During July of 1970, the laser Doppler velocimeter was removed from the Raytheon van and installed in the NASA equipment van in Huntsville. The necessary repairs and maintenance were performed on the laser equipment and a transmission cavity configuration was aligned. Modifications to the NASA van were suggested during this period. During the period, also, Raytheon personnel cooperated in the filming of a NASA movie on Trailing Vortex Detection.

2.1.2 SEPTEMBER - NOVEMBER, 1970

2.1.2.1 Measurements

Raytheon personnel went to Huntsville in September following the moving of the NASA van to a field location. A few modifications were made to the NASA van and the LDV performance was optimized. The laser beam profile and efficiency of the transmitting optics were measured. A series of ground wind data was made using both six-inch and twelve-inch transmitting optics. Range resolution measurements were made with both sets of transmitting optics. Raytheon personnel returned to Sudbury early in November.

2.1.2.2 Laser Beam Profile and Lens Matching

The laser beam diameter was determined by scanning the beam with a small hole in a highly reflective metal plate. The power passing through the hole was measured with a CRL Power Meter. The scan was made in both the vertical and horizontal directions. The diameters of each scan were determined at power points corresponding

to  $1/e^2$  of the peak intensity. These diameters were then averaged to obtain a Gaussian diameter of 5.7 mm in a plane corresponding to the location of the secondary lens of the telescope. The measured profile was also plotted along with a 5.7 mm diameter Gaussian function and found to be in good agreement.

It can be shown that a Newtonian telescope is optimized for energy transmission when

$$\frac{F_1}{F_2} = \frac{\omega'}{\omega}$$

where  $F_1$  = secondary focal length

$F_2$  = primary focal length

$\omega'$  = input Gaussian radius

and

$$\omega = \frac{r_2^2 - r_1^2}{\ln r_2 - \ln r_1}$$

where  $r_2$  = primary radius

$r_1$  = obscuration radius

The transmitting telescope being used during this period had the following parameters:

$$F_2 = 48 \text{ inches}$$

$$r_2 = 3 \text{ inches}$$

$$r_1 = 0.5 \text{ inches}$$

$$\omega = 2.2 \text{ inches}$$

The optimum secondary focal length was found to be 2.35 inches, for which the transmitter efficiency is 90 percent. A germanium

lens of 2-inch focal length (transmitter efficiency 86 percent) was available within NASA and it was decided to use it. The same efficiencies apply to the 12-inch diameter 96-inch focal length telescope, assuming the central obscuration is one inch in radius.

2.1.2.3 LDV Resolution Data

Range resolution data were obtained for both 6-inch and 12-inch telescope systems. These data were compared with theoretical expressions previously derived (Final Report, Ground Wind and Wind Tunnel Velocity Measurements, SR70-4145, Volume 1, Contract No. NAS8-21293). This derivation assumes that the laser transmits a beam of Gaussian profile with the  $1/e^2$  intensity point at a radius R. The derivation further assumes that the transmitted beam has no central obscuration and is not truncated around the outside. For a Newtonian transmitter, the central obscuration and outer truncation will cause a deviation from the calculated values.

For an atmosphere that extends from  $L_1$  to  $L_2$ , the signal-to-noise ratio is given by

$$S/N = \frac{\eta P_T \beta(\pi) \lambda}{2 h\nu B} \left\{ \begin{aligned} & \tan^{-1} \left[ \frac{\lambda L_2}{\pi R^2} - \frac{\pi R^2}{\lambda f} \left( 1 - \frac{L_2}{f} \right) \right] \\ & - \tan^{-1} \left[ \frac{\lambda L_1}{\pi R^2} - \frac{\pi R^2}{\lambda f} \left( 1 - \frac{L_1}{f} \right) \right] \end{aligned} \right\} \quad (1)$$



where:  $\eta$  = detector quantum efficiency  
 $P_T$  = transmitter power  
 $\beta(\pi)$  = atmospheric backscatter coefficient  
 $B$  = system bandwidth  
 $R$  = transmitter radius  
 $f$  = range to focused spot of beam

For a symmetrical system, where

$$L_2 = f + \frac{\Delta L}{2} \quad (2a)$$

$$L_1 = f - \frac{\Delta L}{2} \quad (2b)$$

substituting equation (2a) and equation (2b) into equation (1) yields

$$S/N = \frac{\eta P_T \beta(\pi) \lambda}{2 h \nu B} \left\{ \begin{aligned} & \tan^{-1} \left[ \frac{\lambda f}{\pi R^2} + \frac{\lambda \Delta L}{2\pi R^2} + \frac{\pi R^2 \Delta L}{2\lambda f^2} \right] \\ & - \tan^{-1} \left[ \frac{\lambda f}{\pi R^2} - \frac{\lambda \Delta L}{2\pi R^2} - \frac{\pi R^2 \Delta L}{2\lambda f^2} \right] \end{aligned} \right\} \quad (3)$$

or

$$S/N \propto \tan^{-1} \left[ \frac{\lambda f}{\pi R^2} + \frac{\lambda \Delta L}{2\pi R^2} + \frac{\pi R^2 \Delta L}{2\lambda f^2} \right] - \tan^{-1} \left[ \frac{\lambda f}{\pi R^2} - \frac{\lambda \Delta L}{2\pi R^2} - \frac{\pi R^2 \Delta L}{2\lambda f^2} \right] \quad (4)$$

The value of R is obtained from the measured value of the laser beam diameter and the relative focal lengths of the primary and secondary of the telescopes. The Gaussian radius of the laser beam is 2.85 mm. For the two telescopes, this corresponds to transmitted Gaussian radii of 2.64 inches for the six-inch F/8 system and 5.38 inches for the twelve-inch, F/8 system, both using a two-inch focal length secondary.

The theoretical and experimental values are plotted for comparison in Figure 2-1 for

$$f = 73 \text{ feet}$$

$$\lambda = 10.6 \times 10^{-4} \text{ cm}$$

$$R = 2.64 \text{ in. and } 5.38 \text{ in.}$$

as a function of  $\Delta L$ . The experimental curves were scaled to make their asymptotes near the value of  $\pi$  expected on the basis of Equation 4. The curves clearly show the increase in the "depth of field" resulting from truncation of the Gaussian beam.

### 2.1.3 DECEMBER, 1970

In December R. Schaaf went to Huntsville for ten days to assist in taking ground wind data and final preparation before packing the van for shipment to Colorado.

## 2.2 MEASUREMENTS AT COLORADO STATE UNIVERSITY SITE

### 2.2.1 FEBRUARY, 1971

In February, Raytheon personnel went to the CSU site to assist in set up and operation of the ground wind system. Maintenance was performed on the laser and a new higher voltage transformer installed. The twelve-inch system was aligned and returns were obtained in the reflection cavity configuration. Raytheon personnel

2-6

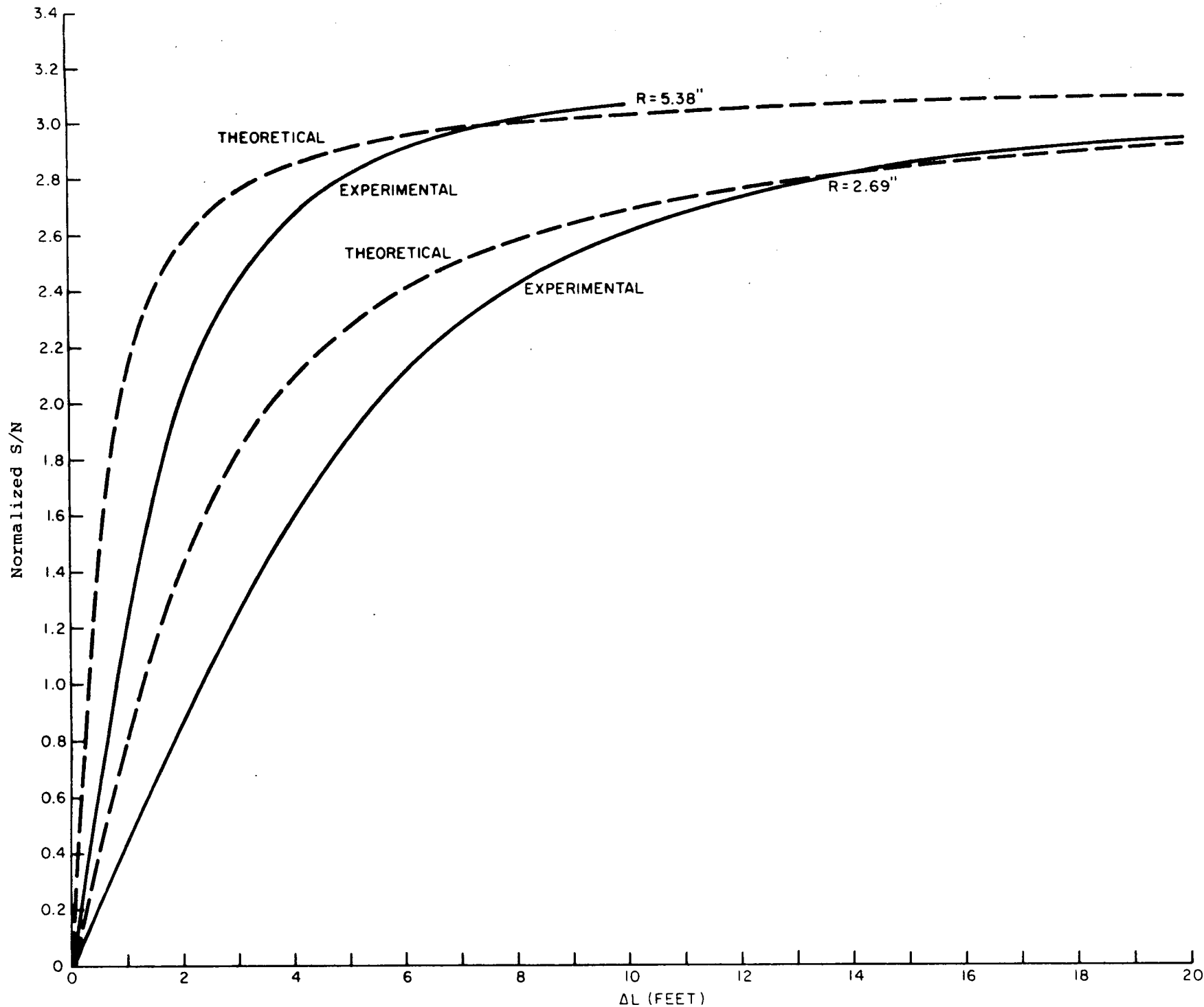


Figure 2-1. Range Resolution (f - 73 feet)

RAYTHEON COMPANY  
EQUIPMENT DIVISION



assisted CSU personnel in preparing for data measurements and instructed them in operation of the LDV.

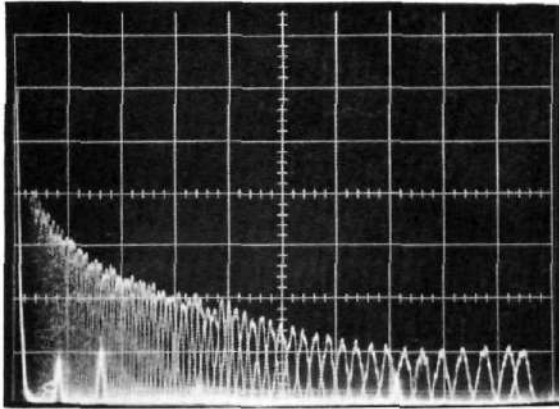
### 2.2.2 MARCH - APRIL, 1971

Dr. W. Keene and C. Miller visited the CSU site from 23 March to 6 April. During this time repairs were made to the laser vacuum systems and all the system optics were realigned. Measurements were made on the system characteristics as set up in the NASA van and a series of measurements were made on front cavity and back cavity configurations using spinning wheels and ground wind signals were recorded at up to 36 MPH.

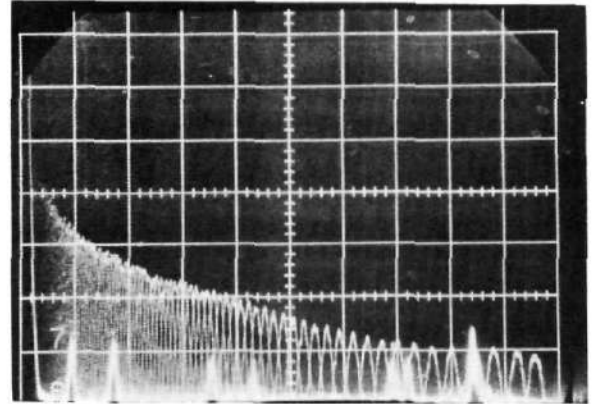
The frequency response of the Perry amplifier was checked with a 50  $\Omega$  termination and found to be flat to 10 MHz. Operation in the system, however, showed that there was a roll-off of about 10 dB between 1 MHz and 10 MHz, as determined by measuring detector g-r noise. In addition, there were variations in sensitivity between 1 MHz and 20 MHz. When the Perry Amplifier was removed from the system electronics the roll-off and sensitivity variations disappeared. It is thought therefore that these characteristics may be the result of the use of 35 feet of 70  $\Omega$  RG59U between amplifier and spectrum analyzer. As a consequence of this variation, interpretation of several cavity gain measurements is not very meaningful insofar as confirming the  $1/f^2$  fall-off expected.

Front and rear cavity measurements were made utilizing three types of spinning wheel surfaces: (1) a scribed plexiglass disk; (2) a plexiglass disk with a roughened surface, and (3) a felt-covered disk. The results for the plexiglass disks are shown in Figure 2-2, which also demonstrates the variations in sensitivity resulting when the amplifier is used.

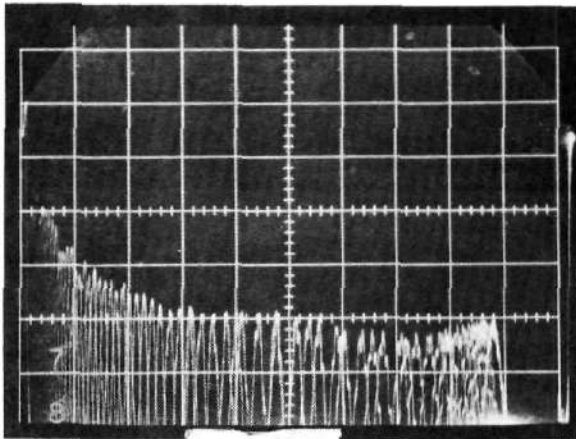
In the case of the felt-covered wheel measurements, two different cables were used in the two positions to connect the amplifier to the spectrum analyzer and this may account for the 10



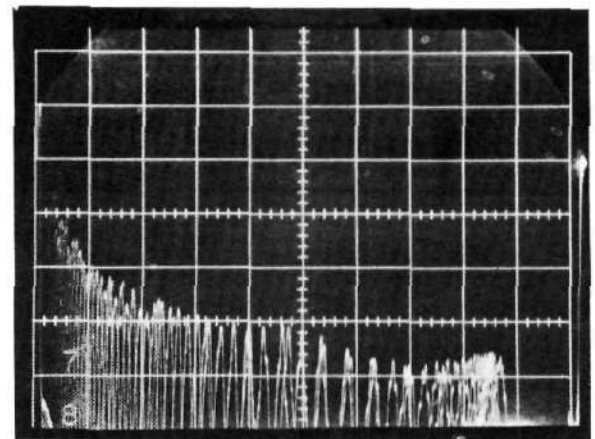
a) Front Cavity  
Scribed Plexiglass Disk  
No Amplifier  
1.4 MHz/Div.  
10 dB/Div.



b) Rear Cavity  
Scribed Plexiglass Disk  
No Amplifier  
1.4 MHz/Div.  
10 dB/Div.



c) Front Cavity  
Roughened Plexiglass Disk  
Perry Amplifier  
2 MHz/Div.  
10 dB/Div.



d) Rear Cavity  
Roughened Plexiglass Disk  
Perry Amplifier  
2 MHz/Div.  
10 dB/Div.

Figure 2-2. Signal Returns from Spinning Disks

dB difference. The relatively small difference between the results of the measurements on the plexiglass disks could well be due to variations in placement of the detector.

Measurements were made at various focal ranges during a snow storm. The photographs are shown in Figures 2-3 and 2-4. Figure 2-3 was obtained using the full 12-inch aperture of the telescope, while in Figure 2-4 the telescope was apertured down to 6 inches. The signal obtained with the twelve-inch aperture fell much more rapidly than expected theoretically. For a transmitted beam with a Gaussian distribution and a uniform atmospheric target, the signal variation over all ranges is not expected to exceed 3 dB. It is not possible on the basis of this measurement, however, to determine the source of the departure from theory.

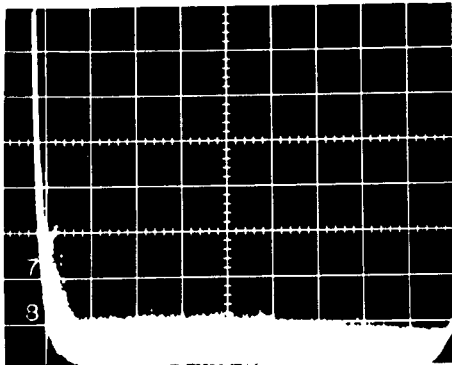
Strong winds occurred on several occasions during the measurements at CSU. On March 31, the winds reached 60 MPH with gusts to 90 MPH. Still photographs (see Figure 2-5) were taken of the analyzer display and show radial components in the range of 25 - 35 MPH with S/N ratios of 10 - 15 dB. Films taken of an oscilloscope display show radial components in the 50 - 60 MPH range, but are limited in use because the short persistence of the screen resulted in only brief portions of the spectrum being displayed in any one frame.

It was not possible to align the LDV beam with the wind since only the lower mirror on the tower was being used. In the high wind conditions it was not possible to align the upper mirror which would have permitted measurements of the full wind velocity.

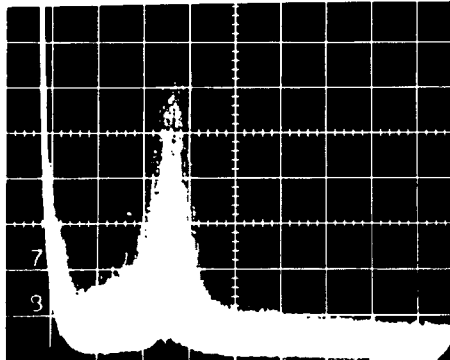
Shortly before leaving CSU, the laser was overhauled. A new salt flat was installed, the bore was realigned, mirrors were cleaned and realigned and the laser power was brought back up to the 26 - 27 watt level.

CLEAR AIR RETURNS - Ft. Collins, Colorado  
12" OPTICAL SYSTEM.

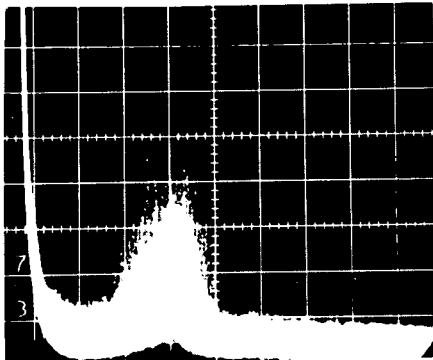
16964- 65



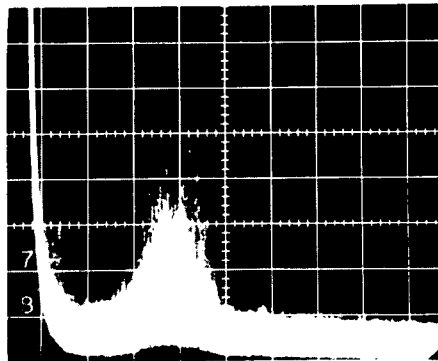
NNSE



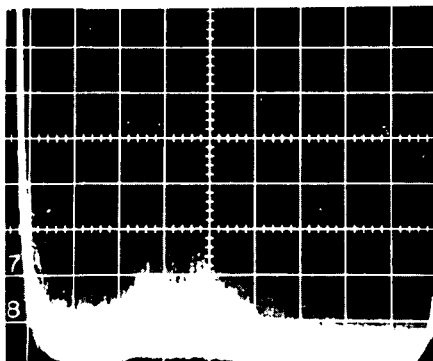
100 FT RANGE



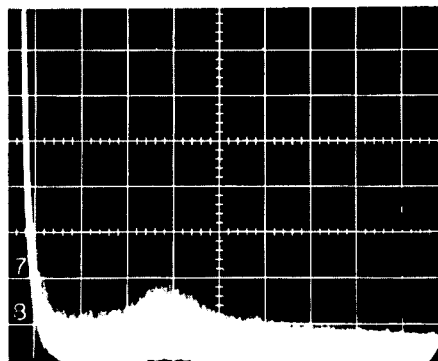
300 FT RANGE



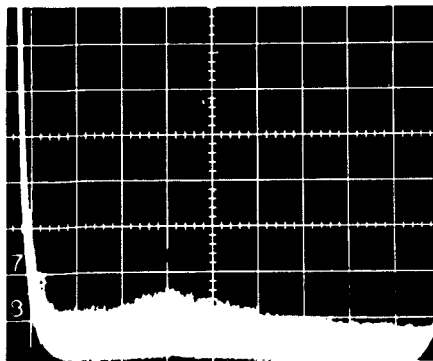
400 FT RANGE



800 FT RANGE



1600 FT RANGE



SNOW

SNOW PARTIALLY  
COVERING OUTSIDE  
MIRROR!

10 SEC EXPOSURES  
30 SWEEPS/SEC.

580 PARTICLES/LITER

30 KHz BANDWIDTH  
0.1 MHz / DIV (HORIZ)

LINEAR SCALE  
10 KHz VIDEO FILTER  
2 μS / DIV SCAN RATE

LASER POWER = 20 W

12 IN OPTICAL  
TELESCOPE!  
NO APERTURES!

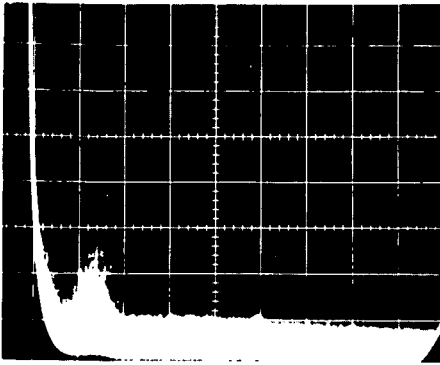
3 APRIL 1971

Christopher R. Weller

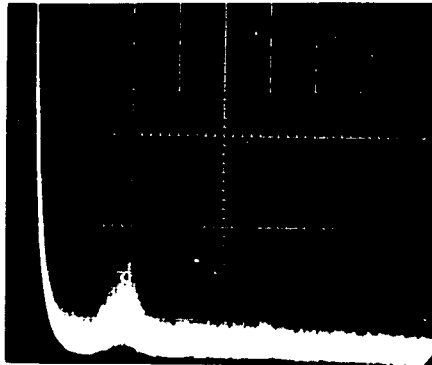
Figure 2-3. Snow Returns at Various Ranges  
12-Inch Transmitter

16964- 64

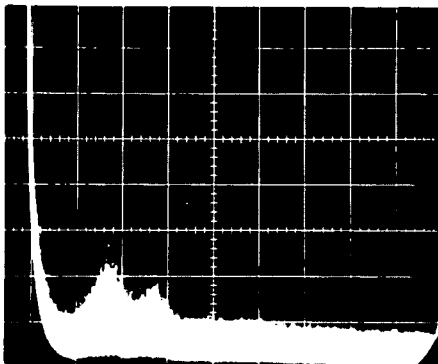
CLEAR AIR RETURNS - Ft. Collins  
12" TELESCOPE APERTURED TO 6"



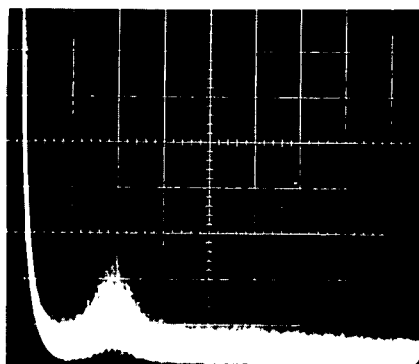
100 FT RANGE



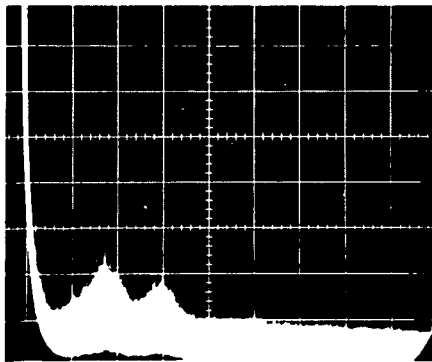
200 FT RANGE



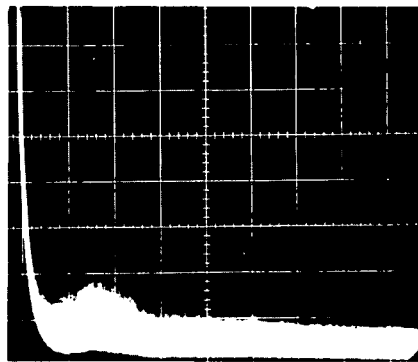
400 FT RANGE



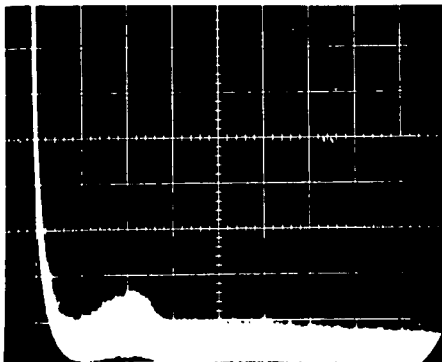
800 FT RANGE



1600 FT RANGE



1600 FT RANGE



∞ RANGE

SNOW

OUTSIDE WINDOW WEST

10 SEC. EXPOSURE

20 SCANS/SEC.

500 PARTICLES/MTX.

30 kHz BANDWIDTH

0.1 MHz/DIV (VIDEO)

LINEAR SCALE

10 kHz VIDEO FILTER

2ms/DIV SCAN

LASER POWER = 20 W

6" APERTURE IS  
FRONT OF TELESCOPE  
OUTPUT LIMITS  
OUTPUT POWER  
FROM THE  
TELESCOPE!

3 APRIL 1971

*Christopher R. Walker*

Figure 2-4. Snow Returns at Various Ranges  
12-Inch System with 6-Inch Aperture



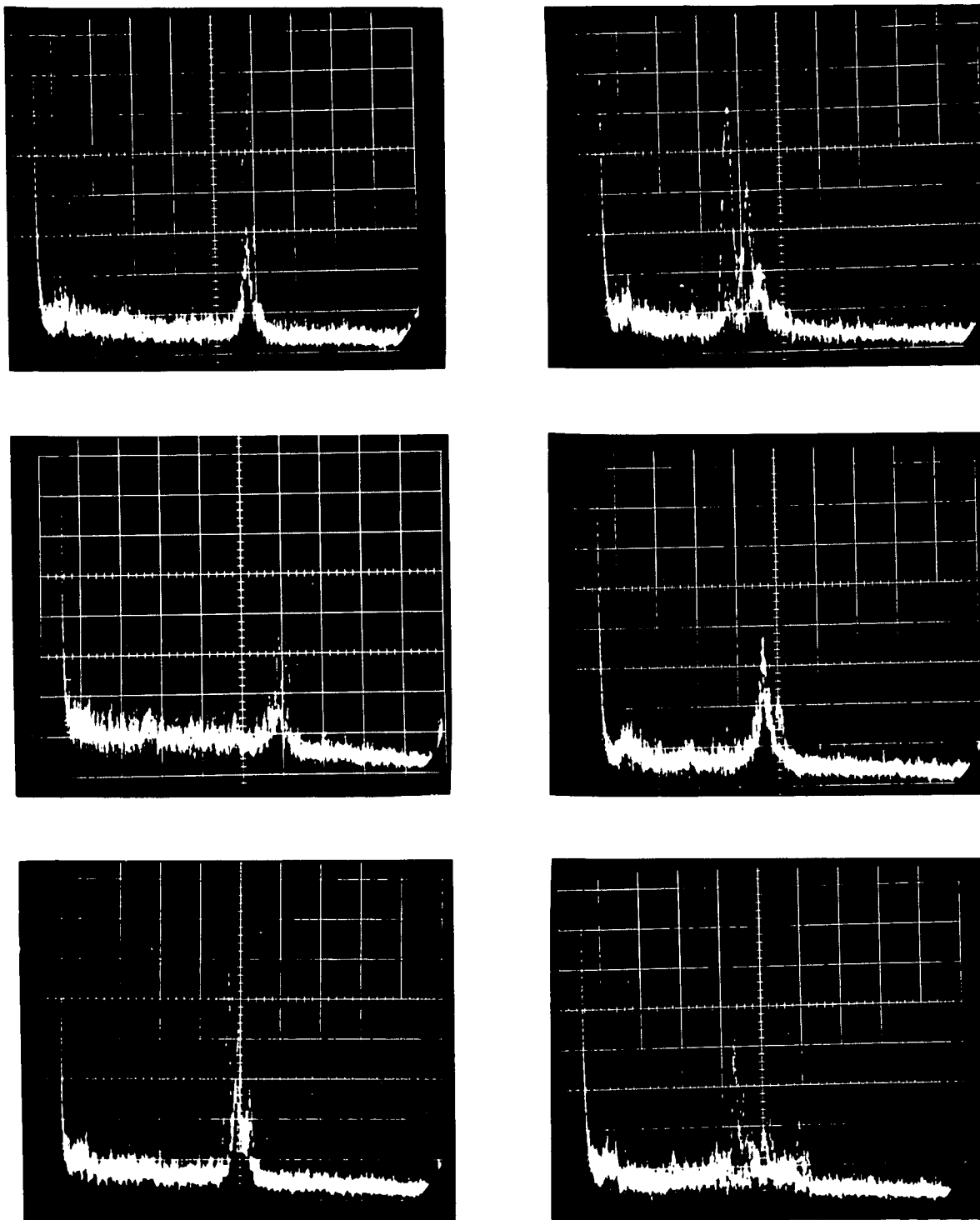


Figure 2-5. Ground Wind Returns, Ft. Collins, Colorado, 31 March 1971  
0.5 MHz per Division  
5 MHz Full Scale  
60 Miles per hour Full Scale

SECTION 3

GROUND WINDS FREQUENCY TRACKER

3.1 CHARACTERISTICS

A special purpose signal processor, a Wide Band Frequency Tracker, has been designed and built for the purpose of tracking ground wind signals generated from a 10.6 micron CO<sub>2</sub> Laser Doppler Velocimeter system. The ground wind velocity and turbulence characteristics to which the electronic read-out system was designed are as follows:

Mean Wind Velocity Range:	0.5 ft/second to 100 ft/second
Gustiness:	Turbulence fluctuations of the order of 20% to 50% about the mean velocity at rates of 20 Hz (inertial subrange) and larger
Acceleration:	Typically 2.25 ft/sec <sup>2</sup> at 20 ft/second (5% probability)
Power Spectral Density:	Wind energy distributed over a turbulence frequency range from laminar (0 Hz), peak at inertial subrange (20 Hz), through fine viscous dissipation (2 KHz)

The characteristics of the Ground Winds Frequency Tracker, Model 12C, developed to meet these general specifications are as follows:

Tracking Range:	50 kHz - 12 MHz
Frequency Deviation:	
a) Wide Turbulence Mode:	50 kHz bandwidth
	1.5 MHz at a 250 Hz rate
	25 kHz at a 2 kHz rate

b) Narrow Turbulence Mode: 15 kHz bandwidth

0.5 MHz at a 125 Hz rate

7.5 kHz at a 1 kHz rate

Signal Frequency:	0 - 2 kHz
Track Acceleration:	$10^7$ Hz/second, corresponding to a gust acceleration of $160 \text{ ft/sec}^2$
Input Signal Level:	10 db over 50 kHz bandwidth
Signal Drop-outs:	Hold logic adjustable from 1 second to 5 seconds without losing lock
Search Mode:	After losing lock, when signal drop-out time is larger than hold logic, initiates automatic search mode. Sweep-time adjustable from 0.5 seconds to 5 seconds. Will re-acquire LDV Doppler signal and track.

The feature that differentiates this tracker from the one developed for supersonic wind tunnel flow applications is its smaller tracking range and frequency response. However, it has a search mode, which together with the hold and track modes, makes it a very versatile and useful instrument to the experimental meteorologist. An Operating Manual for the Frequency Tracker, Model 12C, has been prepared under separate cover. It contains operating and adjustment instructions, a complete set of schematics, and a detailed description of the instrument.

A major problem in the Tracker design was the combination of the IF filters and the frequency discriminator. The narrow filter bandwidth in conjunction with the relatively low sensitivity of the discriminator creates an ambiguous discriminator output voltage vs. frequency characteristic. The problem is caused by a shift of the discriminator center frequency for low input amplitudes.

In Figure 3.1 the original discriminator characteristic at 30 MHz center frequency is shown. It is very linear and has a single, non-redundant zero-crossing level which generates a symmetrical response in its demodulation characteristic. When the discriminator is band-limited by a sharp 50 kHz wide crystal filter, the characteristic shown in Figure 3.2 is obtained. This ambiguous characteristic is due to the variation of the discriminator S-curve sensitivity, at very low input signal levels, which in turn are encountered at the sharp skirts of the filter. Thus, as shown in Figure 3.2, two sharp spikes appear at the skirts of the band limit. These, as well as the resultant change in slope, cause an ambiguous discriminator response. With a 15 kHz wide crystal-filter, this phenomenon is aggravated. The sharp band-limiting of the discriminator creates an oscillation in the tracker lock-on mechanism, with the result that proper operation in the narrow-mode of turbulence is not possible. The problem was adequately solved and the effect was reduced considerably by re-aligning the discriminator and adding an external zero adjustment. Figure 3.3 shows the resultant 50 kHz filter-discriminator characteristic. Figure 3.4 shows the same for the narrow turbulence, 15 kHz filter bandwidth case. The problem of unstable tracking caused by the redundancy in the original characteristic has been solved for the wide-mode turbulence at 50 kHz. However, in the narrow turbulence mode, as seen in Figure 3.4, the problem is still noticeable and results in a slightly degraded performance. The ultimate solution to this problem will be to replace the original Foster-Seely type electronic discriminator with a crystal-discriminator, that inherently has a higher sensitivity and narrower bandwidth.

NOT REPRODUCIBLE

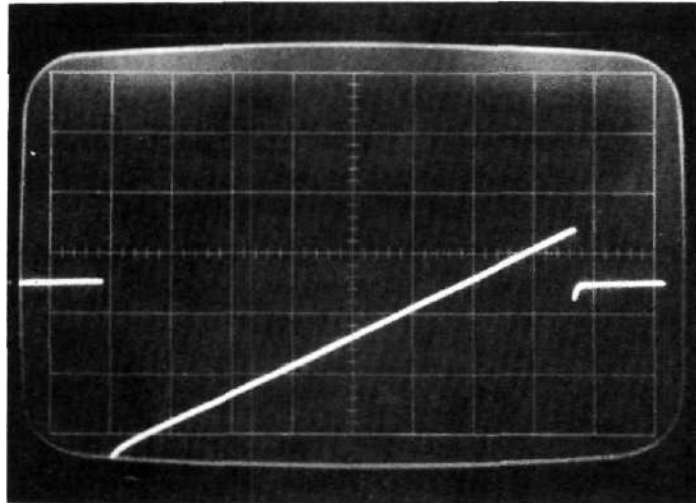
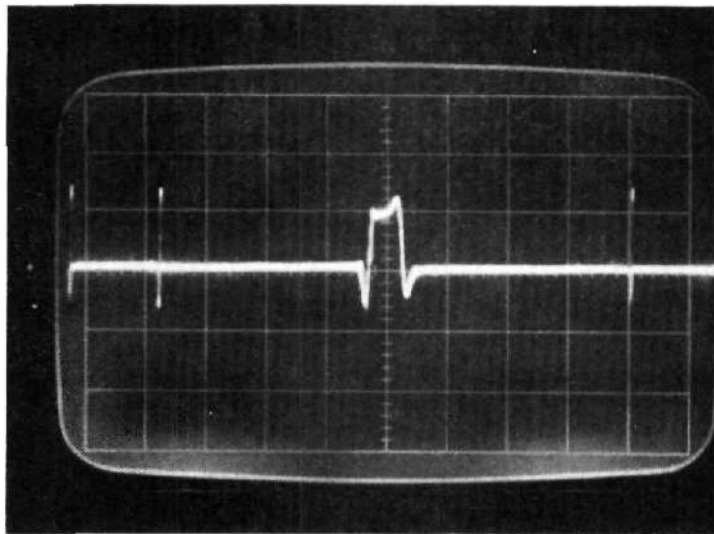
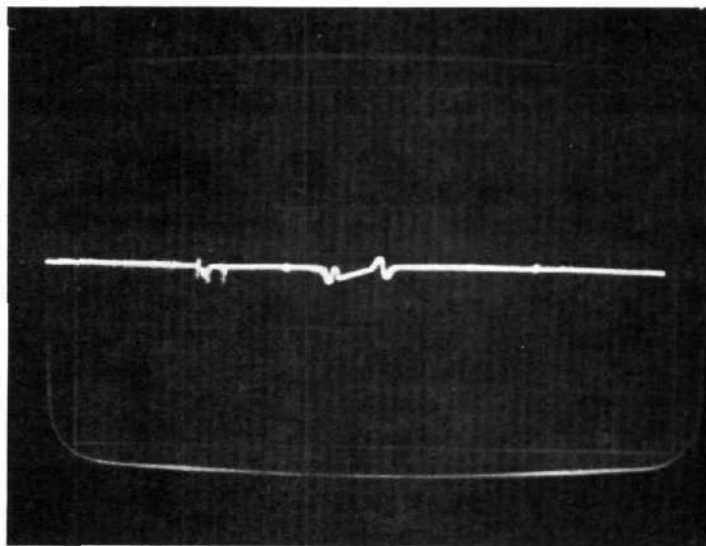


Figure 3.1 Foster-Seely Discriminator S-Characteristic



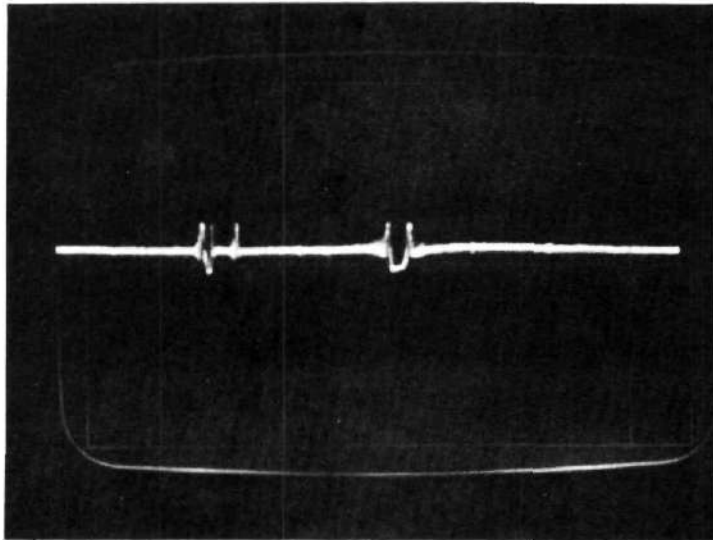
Vert: 50 mV/div  
Hor:  $\approx$  100 kHz/div

Figure 3-2. Wide Filter/Original Discriminator  
Discriminator Zero Not Adjusted



Vert: 50 mV/div  
Hor: 100 kHz/div

Figure 3-3. Wide Filter/Realigned Discriminator  
With Zero Adjustment



Vert: 50 mV/div

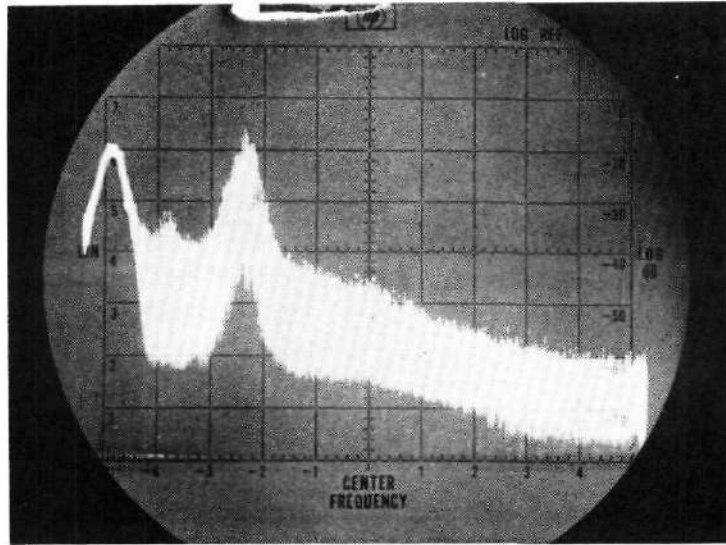
Hor: 100 kHz/div

Figure 3-4. Narrow Filter/Realigned Discriminator  
With Zero Adjustment

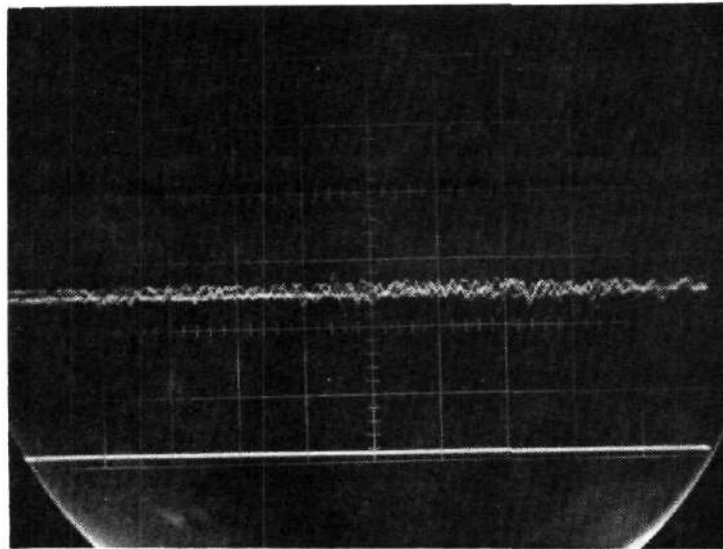
### 3.2 OPERATION OF THE MODEL 12C FREQUENCY TRACKER

After completion of tests and calibration the Frequency Tracker was operated on real 10.6 micron ground wind signals available on tape and derived from initial tests of the CO<sub>2</sub> Laser Doppler Velocimeter performed at Huntsville, Alabama. It performed extremely well and tracked the signal throughout the 15-minute recording time. At all times the Track, Hold, and Search functions of the device performed well. Figures 3.5 through 3.8 show the LDV signal as appearing on a spectrum analyzer and the corresponding Tracker video input, demodulated AC Tracker output and drop-out indicator for wind speeds at 4.3, 3.3, 2.7, and 2.3 ft/second. It is interesting to compare Figures 3.5 and 3.8 for winds at 4.3 ft/second and 2.3 ft/second. In the former, a very good signal-to-noise ratio, 22 db over a 30 kHz bandwidth, and a relatively narrow Doppler spectrum generates a clear video signal and a relatively small RMS fluctuation in the Tracker AC output, compared to the latter in Figure 3.8, where the signal-to-noise ratio of the LDV signal is at 10 db and the RMS AC output of Tracker larger, due to a higher level of turbulence in the signal. The drop-out indicator, in both cases, indicates a continuous acquisition mode. If either the signal level drops out or else the signal-to-noise ratio is reduced below 8 db in 50 kHz, the drop-out indicator will register a level-change, to indicate that the signal quality is not trackable. By examining, in turn, Figures 3.6 and 3.7, one observes a reduction of the signal-to-noise ratio, as seen both on the spectrum analyzer as well as the tracker video input trace. The tracker, however, continues to demodulate properly, and yields the AC voltage analog to the velocity fluctuations within the resolution volume of the LDV.



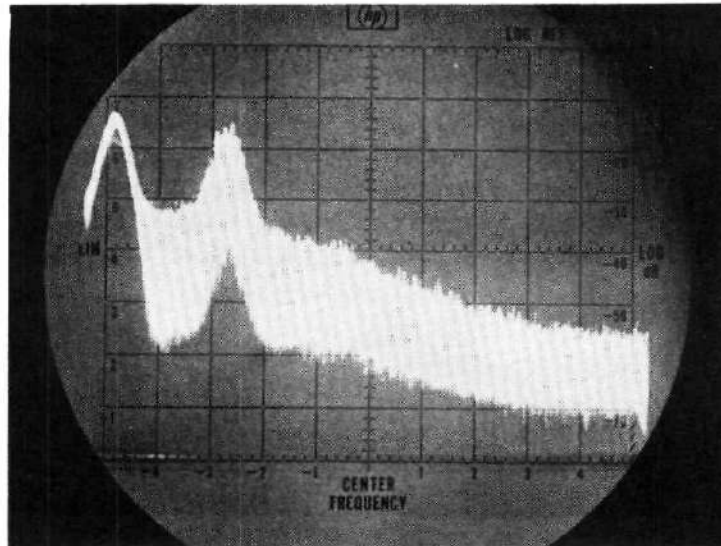


Horizontal Scale: 100 kHz/div.  
BW : 30 kHz  
S/N : 22 db

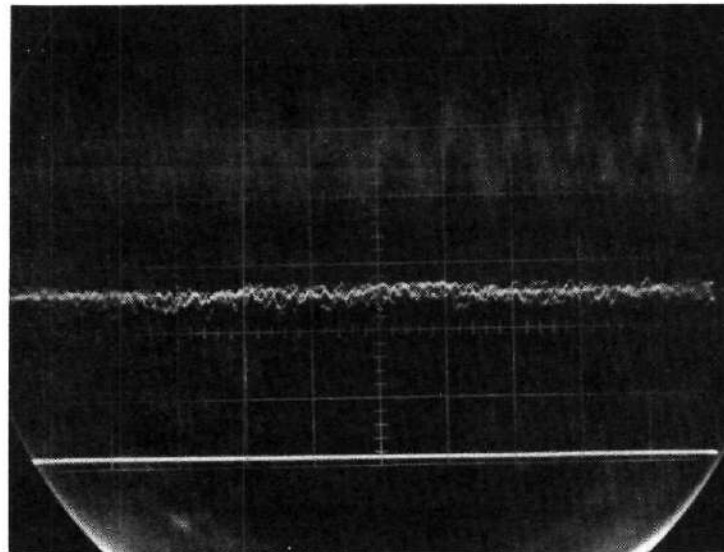


Top: Tracker Video Input  
5  $\mu$ sec/cm, 50 mV/cm  
Middle: Demodulated AC Tracker  
Output--2 msec/cm, 50 mV/cm  
Bottom: Drop-out Indicator

Figure 3-5. 4.3 ft/second Ground Wind Signal

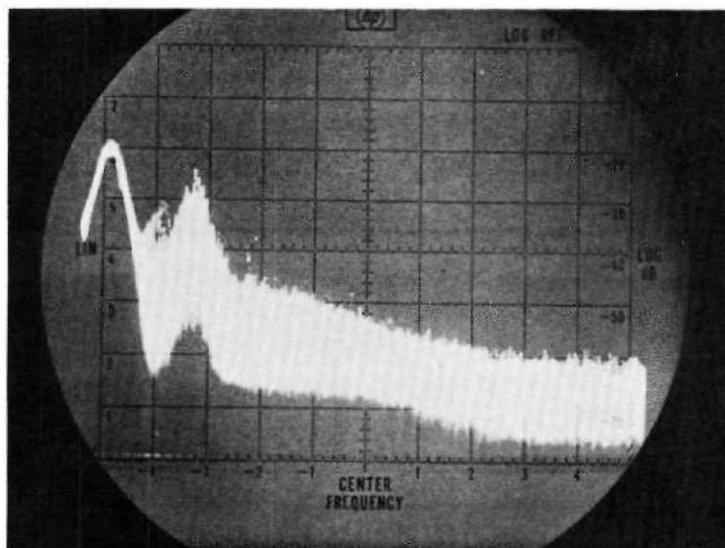


3.5 ft/second  
Horizontal Scale: 100 kHz/div.  
BW : 30 kHz  
S/N : 16 db

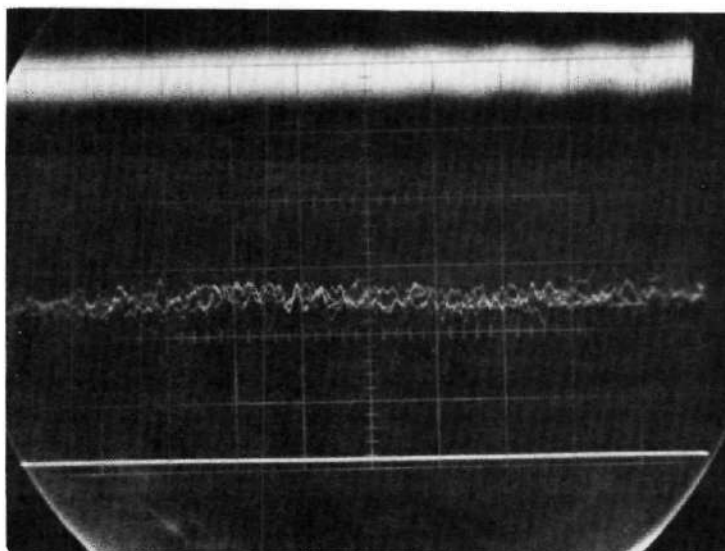


Top: Tracker Video Input  
Middle: Demodulated AC Tracker Output  
Bottom: Drop-out Indicator

Figure 3-6. 3.3 ft/second Ground Wind Signal

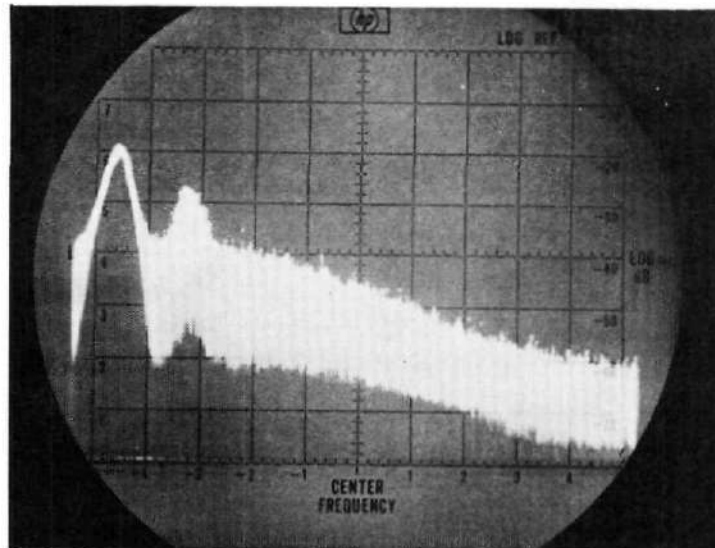


Horizontal Scale: 100 kHz/div.  
BW : 30 kHz  
S/N : 12 db

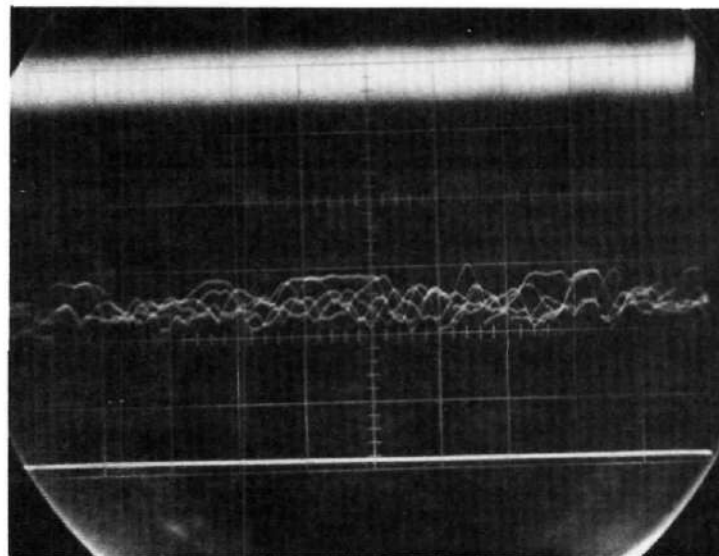


Top: Tracker Video Input  
Middle: Demodulated AC Tracker Output  
Bottom: Drop-out Indicator

Figure 3-7. 2.7 ft/second Ground Wind Signal



Horizontal Scale: 100 kHz/div.  
BW : 30 kHz  
S/N : 10 db



Top: Tracker Video Input  
Middle: Demodulated AC Tracker Output  
Bottom: Drop-out Indicator

Figure 3-8. 2.3 ft/second Ground Wind Signal

After delivery of the Frequency Tracker in Huntsville, the unit was shipped by NASA/MSFC to Colorado State University for inclusion in tests to be conducted on the LDV field range. An oscillation developed in the AGC loop. The problem was later tracked down to the faulty operation of two Model  $\mu$ A715 Fairchild Operational Amplifiers, which were found to be prone to spurious oscillations. These oscillations could have been generated by some connections that got loose in the amplifier base construction. The units were replaced by Raytheon Model RM101TE operational amplifiers, and the oscillations eliminated from the AGC loop.

## SECTION 4

## CONCLUSIONS AND RECOMMENDATIONS

The LDV as presently constituted provides good ground wind signals under a variety of conditions. The loss in sensitivity of the cavity systems at high frequency appears to be at least partly compensated by an increase in the scattering cross section of the atmosphere due to the raising of dust.

On the basis of experiments with the spinning disks, the difference in sensitivity between front and rear cavity does not appear to be great at frequencies below 10 MHz. This is in agreement with analyses which have been done in the past showing that for low frequencies the same signal power is available in the two modes of operation. The same analysis shows that the transmission cavity should be 3 dB below the reflection cavity at 4.5 MHz; however on the present LDV system, this difference appears at a frequency of about 10 MHz when using a spinning disk target. Since signal frequencies are not expected to approach 10 MHz, the reflection cavity mode has only a small advantage over the transmission mode.

Relatively few system improvements are possible on the present system. It should be possible to reduce the 20 percent loss occurring in the germanium secondary lens. With the six-inch system, the transmission efficiency (using one pointing mirror) was 70 percent exclusive of the losses as measured for the germanium lens and as calculated for mismatch in the telescope. It should be possible to raise this value by reducing the number of reflecting surfaces and by replacing the aluminum coatings with gold surfaces.

It is probable that for signal frequencies in excess of 1 MHz, an increase in signal level could be achieved by using a Mach-Zehnder

interferometer instead of the cavity mode. This configuration, however, would require greater alignment stability than the present system demonstrates and would not seem to be necessary in view of the signal amplitudes now being obtained on all but the clearest days.

Prior to the collection of additional data, the post amplifier electronics should be corrected to provide a uniform frequency response. The roll-off which was characteristic during the March-April measurements could cause signal dropout in processing schemes in which a signal threshold is established instead of a S/N threshold. This would lead to an incorrect assessment of the capabilities of the LDV.